

# Plasma-Driven in Situ Production of Hydrogen Peroxide for Biocatalysis

Abdulkadir Yayci,<sup>[a]</sup> Álvaro Gómez Baraibar,<sup>[b]</sup> Marco Krewing,<sup>[a]</sup> Elena Fernandez Fueyo,<sup>[c]</sup> Frank Hollmann,<sup>[c]</sup> Miguel Alcalde,<sup>[d]</sup> Robert Kourist,<sup>[b, e]</sup> and Julia E. Bandow<sup>\*[a]</sup>

Peroxidases and peroxygenases are promising classes of enzymes for biocatalysis because of their ability to carry out one-electron oxidation reactions and stereoselective oxyfunctionalizations. However, industrial application is limited, as the major drawback is the sensitivity toward the required peroxide substrates. Herein, we report a novel biocatalysis approach to circumvent this shortcoming: in situ production of H<sub>2</sub>O<sub>2</sub> by dielectric barrier discharge plasma. The discharge plasma can be controlled to produce hydrogen peroxide at desired rates, yielding desired concentrations. Using horseradish peroxidase,

it is demonstrated that hydrogen peroxide produced by plasma treatment can drive the enzymatic oxidation of model substrates. Fungal peroxygenase is then employed to convert ethylbenzene to (*R*)-1-phenylethanol with an *ee* of >96% using plasma-generated hydrogen peroxide. As direct treatment of the reaction solution with plasma results in reduced enzyme activity, the use of plasma-treated liquid and protection strategies are investigated to increase total turnover. Technical plasmas present a noninvasive means to drive peroxide-based biotransformations.

## Introduction

Cold plasmas have a variety of different applications, ranging from surface preparation in material sciences to the treatment of skin infections in plasma medicine.<sup>[1–3]</sup> In general, plasmas are generated by accelerating free electrons through application of an electric field to ambient air or a defined gas mixture.

Collisions of high-temperature electrons with atoms or molecules in the gas phase lead to the formation of excited species, radicals, and metastables, which in turn react to form other species. For ambient air, over 600 different reaction mechanisms are postulated.<sup>[4]</sup> Because the electric field provides the light electrons with high kinetic energy, but not the heavier particles, the overall temperature of the plasma is ambient (hence the term non-thermal plasma). The plasma-generated species as well as the UV photons stemming from the relaxation of excited species can interact with gases or liquids exposed to the plasma. One of the species generated in high amounts in plasma-treated liquids is hydrogen peroxide (H<sub>2</sub>O<sub>2</sub>),<sup>[5]</sup> which can be a valuable oxidant for enzymatic conversions.

Peroxidases and peroxygenases are heme-containing enzymes, which, upon activation by H<sub>2</sub>O<sub>2</sub>, can perform a multitude of natural functions, for example, condensation of biopolymers,<sup>[6]</sup> immune defense,<sup>[7]</sup> or detoxification of highly reactive H<sub>2</sub>O<sub>2</sub>.<sup>[8]</sup> However, peroxidases, which perform one-electron oxidations, and especially peroxygenases (performing both one-electron oxidations and, most interestingly, two-electron oxidation reactions) are also remarkable enzymes for different biotechnological purposes. In particular, the two-electron C–H oxyfunctionalization reactions performed by peroxygenases are attracting great interest in synthetic chemistry.<sup>[9]</sup> Nevertheless, the use of these biocatalysts on a larger scale is challenging, mainly because the substrate H<sub>2</sub>O<sub>2</sub> also leads to inactivation of the enzymes if present at high concentrations.<sup>[10]</sup> In a commercial setting, this would require enzyme replacement after a few reaction cycles or would lead to strong dilution of the reaction solution if H<sub>2</sub>O<sub>2</sub> was added at low concentrations. Both strategies are typically hardly profitable. An alternative to


[a] A. Yayci, M. Krewing, J. E. Bandow  
Applied Microbiology  
Faculty of Biology and Biotechnology  
Ruhr University Bochum  
Universitätsstraße 150, 44780 Bochum (Germany)  
E-mail: julia.bandow@rub.de


[b] Á. G. Baraibar, R. Kourist  
Microbial Biotechnology  
Faculty of Biology and Biotechnology  
Ruhr University Bochum  
Universitätsstraße 150, 44780 Bochum (Germany)

[c] E. F. Fueyo, F. Hollmann  
Department of Biotechnology  
Delft University of Technology  
Van der Maasweg 9, 2629 HZ Delft (The Netherlands)

[d] M. Alcalde  
Department of Biocatalysis  
Institute of Catalysis and Petrochemistry (CSIC)  
Campus Cantoblanco, 28049 Madrid (Spain)

[e] R. Kourist  
current address: Institute for Molecular Biotechnology  
Graz University of Technology  
Petersgasse 14, Graz (Austria)

 Supporting Information and the ORCID identification number(s) for the author(s) of this article can be found under:  
<https://doi.org/10.1002/cssc.201903438>.

 © 2020 The Authors. Published by Wiley-VCH Verlag GmbH & Co. KGaA. This is an open access article under the terms of the Creative Commons Attribution Non-Commercial License, which permits use, distribution and reproduction in any medium, provided the original work is properly cited and is not used for commercial purposes.

using stock solutions is the generation of  $\text{H}_2\text{O}_2$  in situ. To this effect, several different strategies have been developed, such as the use of enzyme cascades,<sup>[11,12]</sup> light-activated flavins,<sup>[13–15]</sup> or photocatalysts.<sup>[16–18]</sup> All these strategies require the addition of extra components to the reaction, incurring additional costs, especially in the case of enzymes and flavins. Another approach uses immersed electrodes and electrochemistry to produce  $\text{H}_2\text{O}_2$ .<sup>[19–22]</sup> Although this system does not rely on the addition of components to the solution, electrodes are immersed, which may trigger precipitation of buffer salts and enzymes. A noninvasive in situ approach that allows control of  $\text{H}_2\text{O}_2$  levels would present a significant advantage.

Here, we report on the use of a novel, noninvasive approach to fuel  $\text{H}_2\text{O}_2$ -based biotransformations: the in situ generation of  $\text{H}_2\text{O}_2$  using a dielectric barrier discharge (DBD) plasma (Figure 1). The DBD device is operated in a surface discharge

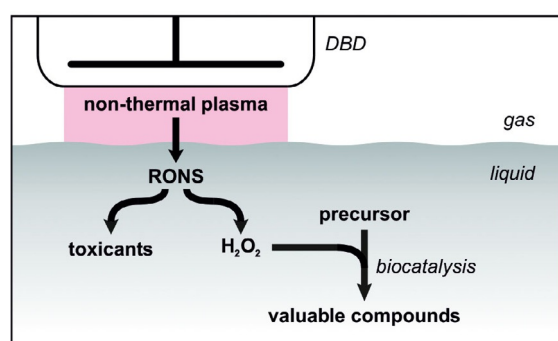


**Figure 1.** General scheme of plasma-driven biocatalysis. A dielectric barrier discharge generates a non-thermal plasma that interacts with the liquid, thus forming reactive oxygen and nitrogen species (RONS), for example, peroxyxynitrite ( $\text{ONOO}^-$ ), superoxide ( $\text{O}_2^-$ ), or  $\text{H}_2\text{O}_2$ . Some of the species can react further to other reactive particles, most of which represent toxicants. Other species such as  $\text{H}_2\text{O}_2$ , however, can serve as reactants to fuel biocatalysis.

mode so that only the plasma comes into contact with the reaction solution. The plasma parameters are readily tunable and can be tailored to the needs of the enzyme employed. For instance, frequency, voltage, and power density influence  $\text{H}_2\text{O}_2$  production and can be adjusted.<sup>[23]</sup> With regard to temperature, the reaction conditions are mild, as the non-thermal plasma used here causes negligible heating.<sup>[24]</sup> A proof-of-principle study was performed with horseradish peroxidase (HRP) and the model substrate guaiacol. The plasma stability of the enzyme, optimal plasma parameters, and plasma-triggered side reactions were investigated. Enzyme protection strategies were tested, including protein immobilization, which, by placing enzymes at a distance from the plasma/liquid interface, protects proteins from the most reactive species. The biotechnological potential with regard to selectivity was evaluated using the evolved recombinant unspecific peroxygenase from *Agroclybe aegerita* (*rAaeUPO*), one of the most promising enzymes for peroxide-dependent oxyfunctionalization chemistry.<sup>[25]</sup>

## Results and Discussion

### Proof of principle

The concept of plasma-driven biocatalysis is illustrated in Figure 1. DBD plasmas induce the formation of reactive oxygen and nitrogen species (RONS), including  $\text{H}_2\text{O}_2$ . Peroxidases or peroxygenases then utilize the supplied  $\text{H}_2\text{O}_2$  to produce valuable products from precursors, that is, oxidized organic substances.

The DBD device used in this study can be ignited in air, eliminating the need for expensive feed gases such as helium or argon, which are commonly used to operate other plasma devices. Also, the source generates  $\text{H}_2\text{O}_2$  in the treated liquid at rates adequate for the enzymes employed here. HRP was used as the model enzyme in the proof-of-principle experiment because it is well-studied, highly stable, and commercially available.<sup>[26–28]</sup> Without further purification ( $RZ > 2.5$ ), HRP was dissolved in phosphate buffer, and, after addition of the chromogenic substrate guaiacol, treated directly with the DBD device operated in ambient air (Figure 2). In the presence of  $\text{H}_2\text{O}_2$ , HRP oxidizes guaiacol to tetraguaiacol, which exhibits  $A_{\text{max}}$  at  $\lambda = 470$  nm. With increasing treatment time,  $A_{470}$  rises, indicating the successful production of tetraguaiacol. Plasma treatment of guaiacol alone or incubation of HRP with guaiacol without plasma treatment did not result in tetraguaiacol production (Figure S1, Supporting Information). Upon use of inactivated HRP (HRP from which heme had been extracted with ethyl acetate), no product was observed either, indicating that enzyme activity is strictly required for guaiacol conversion (Figure S2, Supporting Information). The  $\text{H}_2\text{O}_2$  concentration was measured concomitantly and was found to increase linearly by approximately  $0.1 \text{ mM min}^{-1}$  for the reaction volume tested here. This is in agreement with previous reports on plasma-based  $\text{H}_2\text{O}_2$  production.<sup>[29]</sup>

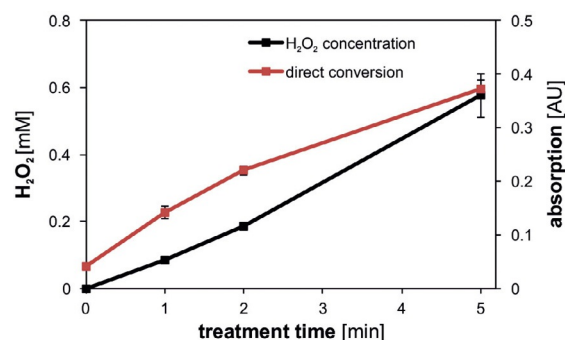


**Figure 2.** Kinetics of  $\text{H}_2\text{O}_2$  accumulation and substrate conversion by HRP during direct plasma treatment with the CINOGY PlasmaDerm DBD device. Samples were placed onto glass slides and treated for the indicated amount of time. Black: 50 mM KPi buffer (100  $\mu\text{L}$ ) was treated with plasma. Immediately after treatment, the samples (20  $\mu\text{L}$ ) were mixed with 180  $\mu\text{L}$  *A. dest.* and  $\text{H}_2\text{O}_2$  concentrations determined using the Spectroquant Hydrogen Peroxide kit (Merck) and photometrical measurements at 455 nm. Red: direct conversion of guaiacol (5 mM) with plasma was achieved by treating KPi buffer (100  $\mu\text{L}$ ) containing  $0.1 \text{ U mL}^{-1}$  HRP. Production of tetraguaiacol was followed at  $\lambda = 470$  nm. The data shown represent means of three independent experiments.

## HRP inactivation mechanisms

Whereas the  $\text{H}_2\text{O}_2$  supply is steady for the treatment times tested, the tetraguaiacol production rate declines after prolonged exposure (Figure 2). The observed decrease in tetraguaiacol production rates at 5 min could be caused by degradation of the enzyme or further modification of the product during plasma exposure. Indeed, the absorption spectrum of the plasma-generated biocatalysis product of guaiacol conversion differed from the product formed with exogenously added  $\text{H}_2\text{O}_2$  (Figure S3, Supporting Information). For alternative HRP substrates, pyrogallol and L-DOPA, we observed oxidation to the final product by plasma treatment even in the absence of enzyme (Figure S4, Supporting Information).

Inactivation of enzymes with the plasma source used here has been shown before, for example, for RNase A, which was fully inactivated after 5 min treatment.<sup>[29]</sup> Activity loss of heme-containing proteins, and specifically HRP, has also been studied,<sup>[30–32]</sup> albeit not with the plasma device used here. Upon treatment with an argon discharge, HRP was fully inactivated within 30 min. However, the plasma device used in this work was specifically designed for use in dermatology<sup>[33]</sup> and could be characterized by slower inactivation kinetics. It is worth mentioning here that the extent of deleterious effects of plasmas are dependent on the enzyme. Some enzymes even exhibited increased activity after plasma treatment.<sup>[34,35]</sup>

To assess HRP inactivation by the plasma treatment performed in this work, we treated HRP with the DBD plasma and determined the activity subsequently *ex situ* with a defined amount of  $\text{H}_2\text{O}_2$  (Figure 3). The HRP activity decreased with increasing plasma treatment time, resulting in only residual activity after 10 min treatment. HRP inactivation was found to be largely independent of protein concentration during treatment (Figure S5, Supporting Information).

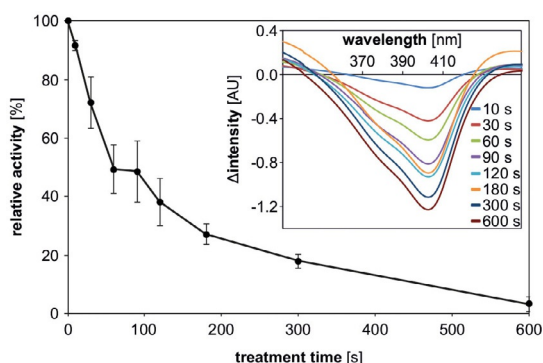


**Figure 3.** HRP inactivation by plasma treatment. Plasma treatment was performed with  $110 \mu\text{L}$  HRP ( $1 \text{ kU mL}^{-1}$ ) in KPi buffer ( $100 \text{ mM}$ ,  $\text{pH } 6.5$ ) without guaiacol. Activity was measured by diluting the treated samples to  $0.1 \text{ U mL}^{-1}$  in KPi buffer including  $5 \text{ mM}$  of guaiacol and subsequent addition of  $\text{H}_2\text{O}_2$  at a final concentration of  $0.25 \text{ mM}$ . Guaiacol conversion was immediately monitored at  $\lambda = 470 \text{ nm}$  and activity calculated from the initial slope during the first 30 s. From the same treated samples, absorption spectra were measured with a 1:5 dilution in KPi. The inset shows the Soret band of HRP with  $A_{\text{max}}$  at  $\approx 403 \text{ nm}$ . Spectra are displayed with the untreated sample as blank, thereby showing a decrease in absorbance at the Soret peak. Data were recorded in triplicate for both activity measurements and spectra.

HRP depends on a heme cofactor for activity, which absorbs at  $\lambda \approx 403 \text{ nm}$  (Soret band). For assessment of the integrity of the heme cofactor, absorption spectra were recorded for the protein samples that were tested for activity (inset of Figure 3). In congruence with previous reports,<sup>[30]</sup> the absorption of the Soret band declined after plasma exposure, indicating that the heme was modified. Heme has been shown to be attacked by ROS, for example,  $\text{O}_2^{\cdot-}$  radicals and  $\text{H}_2\text{O}_2$ ,<sup>[36,37]</sup> both of which represent major components of the discharge and the treated liquid.  $\text{H}_2\text{O}_2$  is needed as a substrate for the peroxidation reaction, but  $\text{O}_2^{\cdot-}$  may only act as toxicant. We attempted to eliminate  $\text{O}_2^{\cdot-}$  radicals using superoxide dismutase A (SodA) from *Escherichia coli*, an enzyme that converts  $\text{O}_2^{\cdot-}$  to  $\text{H}_2\text{O}_2$ . Superoxide dismutases are among the fastest enzymes, operating near the diffusion limit of substrate supply.<sup>[38,39]</sup> SodA was added to the reaction solution prior to plasma treatment, and no difference in the catalytic efficiency of HRP was observed (Figure S6, Supporting Information). Therefore, we conclude that either the concentration of  $\text{O}_2^{\cdot-}$  in plasma-treated samples is insignificant for heme degradation or that SodA is immediately inactivated by plasma-generated species, and thus, cannot provide protection to HRP.

Heme binding can also induce conformational changes in apoproteins.<sup>[40]</sup> It has been shown previously that plasma discharges can impact the structural integrity of proteins,<sup>[29,31,41,42]</sup> so we investigated the structure of HRP upon plasma exposure using circular dichroism (CD) spectroscopy (Figure 4). No conformational changes of HRP were detected even at treatment times of 5 min, which render HRP largely inactive. This indicated that damage to the heme moiety did not negatively affect the HRP structure. The fact that no structural changes were observed also allowed us to draw conclusions on another structural feature, namely, disulfide bonds. HRP contains eight cysteines, all of which are engaged in disulfide bonds, which contribute to the high enzyme stability.<sup>[26]</sup> For RNase A, a highly stable enzyme with four disulfide bonds, oxidation of cysteines to their sulfenic and sulfonic acids was observed upon DBD treatment, which resulted in significant unfolding.<sup>[29]</sup> If such

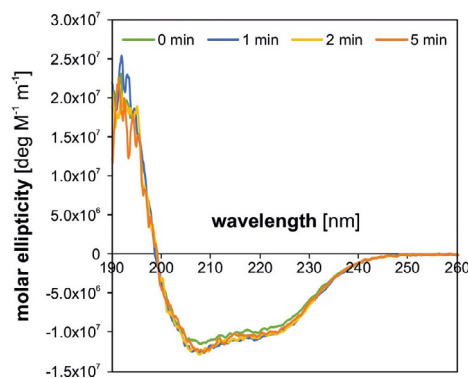


**Figure 4.** CD spectra of HRP after exposure to plasma. HRP ( $110 \mu\text{L}$ ) was treated as described above for activity measurements and diluted 1:5, which corresponds to  $0.2 \text{ mg mL}^{-1}$  for the untreated sample. Immediately after treatment, the sample was transferred to a suitable cuvette and subjected to CD measurements. CD spectra were normalized with respect to protein concentration as determined by the Bradford method.

amino acid modifications also occurred in HRP, they did not seem to affect the overall protein fold.

The specific heme content (heme per protein) of peroxidases is defined by the *RZ* value ( $A_{403}/A_{275}$ ). Because plasma-generated species also absorb in the UV region,<sup>[43]</sup> the specific heme content in this case was calculated as the quotient of  $A_{403}$  and protein concentration as measured by Bradford assay (Figure 5). Dependent on the plasma exposure time, the pro-

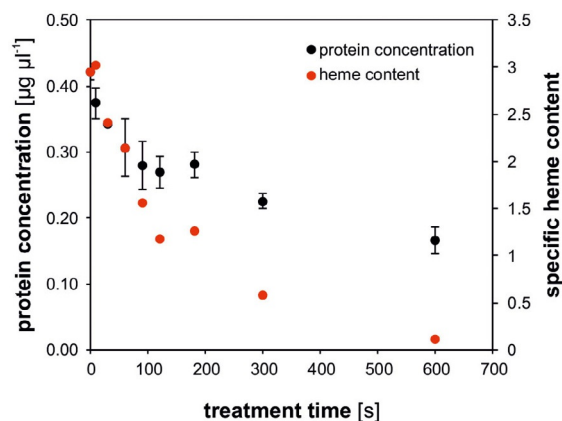


**Figure 5.** Decrease in protein concentration and heme content. Protein concentration was determined using the Bradford method. Specific heme content was set as absorbance at  $\lambda = 403$  (see Figure 3) divided by protein concentration and is displayed in arbitrary units. Protein concentration was determined in triplicate.

tein concentration decreased. This phenomenon was observed previously for HRP as well as other enzymes treated in aqueous solution, for example, hemoglobin, myoglobin, and BSA.<sup>[31,44]</sup> It has been shown that treatment with the plasma source used in this study leads to the cleavage of peptide bonds, and thus, protein degradation.<sup>[44]</sup> This protein degradation was partially inhibited by the addition of mannitol, which had been described as an  $\cdot\text{OH}$  scavenger.<sup>[45]</sup> Protein fragmentation will lead to activity loss. However, because the CD spectra indicated that the structure of the HRP remaining after 5 min treatment was still intact and the rate of heme degradation for HRP exceeded the decrease in HRP concentration, we conclude that heme damage, rather than structural changes or protein degradation, is the primary cause of HRP inactivation.

### Optimizing plasma treatment conditions

For the proof-of-concept study with HRP, the parameters for plasma operation (pulse amplitude 13.5 kV, trigger frequency 300 Hz) were chosen simply by applying the same parameters as in previous studies.<sup>[29,46]</sup> In an effort to optimize operating conditions for the longevity of HRP, a range of amplitudes and frequencies between 11.5 and 17.5 kV and 150 and 700 Hz, respectively, were tested (Figure 6). To this end, HRP activity was measured immediately after 1 min plasma treatment. The activity measurement was decoupled from plasma treatment of the enzyme-containing solution to circumvent the issue of plasma-induced product modification discussed above

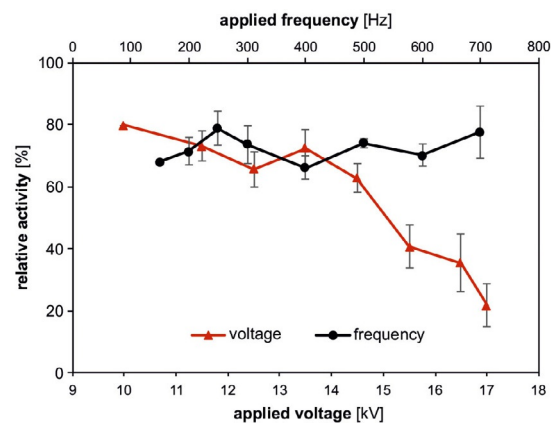


**Figure 6.** Influence of voltage and frequency on HRP after 1 min plasma treatment. HRP was plasma-treated at  $10 \text{ U mL}^{-1}$  for 1 min and activity was subsequently measured ex situ as described above. Untreated samples were set to 100%. The graph shows mean values of three independent replicates.

(Figure 2), which may obstruct interpretation of the results. Changes in trigger frequency showed little to no effect on HRP activity (Figure 6), whereas HRP inactivation increased with increasing applied voltage. A very similar dependence of protein activity on discharge voltage was shown previously for tomato peroxidase, even with similar kinetics, although a different DBD plasma was used.<sup>[47]</sup>

An increase in applied voltage leads to higher electron temperatures in the gas phase, and in turn, increased ROS production, so that a higher density of toxicants is expected in the liquid. It was, for instance, shown previously that  $\cdot\text{OH}$  production in plasma-treated liquid depends on the specific energy transferred, which can be manipulated by altering either the treatment time or the voltage applied.<sup>[23]</sup> Addition of the  $\cdot\text{OH}$  scavenger mannitol during plasma treatment did not have a significant effect on the HRP lifetime (Figure S7, Supporting Information). We speculate that other RONS such as atomic oxygen ( $\cdot\text{O}$ ), UV radiation, and/or the applied electric field<sup>[48,49]</sup> might impact enzyme activity.

Another approach to extending the HRP lifetime was immobilization of the enzyme to nonreactive support beads. Immobilization was achieved by reacting HRP with glutaraldehyde-activated polymer beads. Immobilized HRP exhibited only approximately 10% of the activity of the free enzyme (Figure S8, Supporting Information). However, upon plasma treatment, HRP<sub>immobilized</sub> retained its activity significantly longer. After 5 min treatment, immobilized HRP showed 41.8% activity compared with the untreated HRP<sub>immobilized</sub>, whereas free enzyme activity was reduced to 0.5–10% (results presented in Figure 7 and Figure 3, respectively).

The comparatively high robustness of the immobilized enzyme might be attributed to spatial separation. Most recombination reactions in plasma-treated liquids are thought to occur at or in close proximity to the liquid/gas interface.<sup>[50]</sup> RONS such as singlet oxygen ( $^1\Delta_g\text{O}_2$ ),  $\text{O}_2^{\cdot-}$ , and  $\cdot\text{OH}$  have average diffusion distances in the nanometer to micrometer range.<sup>[51]</sup> The liquid droplets in our experimental setup are approximately 2 mm in height and the protein-loaded beads sink



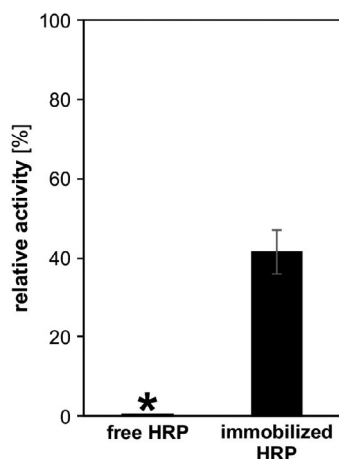


**Figure 7.** Immobilization of HRP protects against plasma-mediated damage. Glutaraldehyde-activated polymethacrylate beads (Relizyme HA403) were incubated with HRP overnight to yield an immobilized HRP solution corresponding to  $20 \text{ U mL}^{-1}$ . For both enzyme formulations,  $100 \mu\text{L}$  was treated at  $13.5 \text{ kV}$  and  $300 \text{ Hz}$ . Free enzyme activity was measured as described above. Activity assays for immobilized HRP were conducted with constant shaking to provide sufficient substrate delivery to the macroscopic beads, using  $5 \text{ mM}$  guaiacol and  $0.25 \text{ mM}$   $\text{H}_2\text{O}_2$ . The displayed relative activities were calculated by relating the activities of treated samples to their respective untreated controls. Data represent means of three replicates.

to the bottom of the sample. This creates a protein-free buffer zone that allows most short-lived toxicants to react and form less harmful species before they can interact with the protein. However, the recombination reactions at the plasma/liquid interface are very challenging to address experimentally. Most studies, therefore, address this question through numerical modelling (reviewed in Ref. [52]). According to the models, many of the reactive species have short lifetimes in the liquid phase, for example, in the nano to microsecond range for  $\cdot\text{OH}$ . Thus, a spatial gradient forms in the liquid phase such that the more reactive species penetrate less deeply before they react further.<sup>[53,54]</sup> The models are congruent with a millimeter of liquid column being sufficient to protect proteins from exposure to the most reactive species.

### Selectivity in plasma-driven biocatalysis

To assess the potential of plasma-driven biocatalysis, we felt it necessary to investigate whether plasma-based  $\text{H}_2\text{O}_2$  production interferes with the stereoselectivity of enzymatic reactions. To this end, the *rAaeUPO* was used, an enzyme capable of performing stereoselective oxidations of hydrocarbons.<sup>[12,55]</sup> For *rAaeUPO*, total turnover numbers (TTNs) of over 10 000 have been reported, indicating its remarkable stability.<sup>[56–58]</sup> As a model reaction we chose the well-characterized oxidation of ethylbenzene to (*R*)-1-phenylethanol, a reaction that would provide proof that a value-adding reaction can be driven by plasma. First,  $\text{H}_2\text{O}_2$  was generated by treating a set volume of  $100 \mu\text{L}$  KPi buffer with plasma for 5 min and then adding it to a solution containing *rAaeUPO* and ethylbenzene (indirect treatment). After 10 min reaction time, another portion ( $100 \mu\text{L}$ ) of treated buffer was added, and after a further

10 min reaction time, another portion ( $100 \mu\text{L}$ ) of treated buffer was added prior to a final 10 min reaction time. Formation of (*R*)-1-phenylethanol was determined, yielding a final concentration of  $0.46 \text{ mM}$  (Table 1).

**Table 1.** Production of (*R*)-1-phenylethanol from ethylbenzene starting with a solution of  $1 \mu\text{M}$  *rAaeUPO* and  $5 \mu\text{L}$  ethylbenzene.<sup>[a]</sup>

Treatment time per increment [min]	Buffer type	concentration [mM]	Final ( <i>R</i> )-1-phenylethanol concentration [mM]	TON
0	KPi	250	0	0
5	KPi	250	$0.46 \pm 0.01$	4576
10	KPi	250	$0.69 \pm 0.25$	6935
15	KPi	250	$0.97 \pm 0.17$	9709
20	KPi	250	$1.38 \pm 0.13$	13787
5	KPi	1000	$0.83 \pm 0.06$	8279
5	KPi	50	$0.7 \pm 0.03$	6993
5	Tris	50	$0.92 \pm 0.01$	9170
5	HEPES	50	$1.35 \pm 0.03$	13493
5	MES	50	$0.78 \pm 0.01$	7831

[a]  $100 \mu\text{L}$  increments of buffer solutions were treated for the indicated amounts of time and added to the reaction solution. After 10 min incubation under agitation, the next increment of treated buffer was added. In total, three increments were added per sample. TON: turnover number. Data represent means and standard deviations of three replicates.

Treatment times for each increment were then varied to change the  $\text{H}_2\text{O}_2$  concentrations. Product formation was linearly correlated with the treatment time. The calculated turnover number of 13787 is indeed of the order of previously reported TTNs for *rAaeUPO*.<sup>[55]</sup> Negative controls without enzyme, plasma treatment, or ethylbenzene did not result in any detectable product formation (Figure S9, Supporting Information). The product was optically pure with *ee* values ranging between 96% and over 99%, which clearly demonstrates that the hydroxylation is indeed an enzymatic reaction (Figure S9). We also tested whether other long-living RONS present in plasma-treated buffer have an impact on *rAaeUPO* activity. The enzyme was added to plasma-treated buffer or to  $\text{H}_2\text{O}_2$  diluted to the same concentration as detected in the plasma-treated sample. After 2 min incubation, the substrate was added and the enzyme activity assay performed using only the  $\text{H}_2\text{O}_2$  already present in the sample (Figure S10, Supporting Information). There was no difference in enzyme inactivation rates, showing that other long-living plasma-induced species such as  $\text{ONOO}^-$  or  $\text{NO}_2$  do not have a significant effect on enzyme lifetime.

Different buffer salts were tested for their influence on the reaction yield. The best results were obtained with HEPES buffer, yielding about twice as much product than with KPi, followed by MES buffer and Tris buffer (Table 1). It has been reported that UV-irradiated HEPES produces  $\text{H}_2\text{O}_2$ , which may be one possible explanation for the observed increase, as the employed plasma source emits UV photons.<sup>[59]</sup> Another possible explanation is that plasma-generated peroxyxynitrite (from the reaction of  $\text{O}_2^-$  and  $\cdot\text{NO}$ ) can react with HEPES to form  $\text{H}_2\text{O}_2$ .<sup>[60]</sup>

Having established that plasma-treated buffer is a suitable source of  $\text{H}_2\text{O}_2$  for biocatalysis with *rAaeUPO*, we investigated

the suitability of *rAaeUPO* for direct plasma-driven biocatalysis. The enzyme (100  $\mu\text{L}$ ; 1  $\mu\text{M}$ ) in 250 mM KPi buffer was mixed with ethylbenzene (5  $\mu\text{L}$ ) and plasma-treated for 5 min, yielding 0.05 mM (*R*)-1-phenylethanol. Compared with supplying  $\text{H}_2\text{O}_2$  from plasma-treated KPi buffer incrementally, plasma-driven biocatalysis gave a yield of 11%, indicating either enzyme inactivation, substrate limitation (the substrate is poorly soluble in aqueous solution and forms an organic phase on top of the reaction solution), or degradation of the product (*R*)-1-phenylethanol by short-lived plasma species. Like HRP, *rAaeUPO* relies on a heme cofactor. The inactivation kinetics of *rAaeUPO* were similar to those of HRP (Figure S11, Supporting Information). The addition of *E. coli* SodA also did not have a significant effect on the lifetime of *rAaeUPO* upon exposure to plasma (Figure S12, Supporting Information). In addition, as for HRP, upon immobilization of *rAaeUPO* using the same carrier, the relative activity after plasma treatment compared with untreated samples was significantly higher than for the free enzyme (Figures S11 and S13 in the Supporting Information). Immobilized *rAaeUPO* retained approximately 39% activity compared with the free enzyme (Figure S14, Supporting Information), indicating that immobilization has less of an impact on enzyme activity than for HRP (approximately 10% activity after immobilization (Figure S8)). However, if immobilized *rAaeUPO* was treated directly in solution in the presence of ethylbenzene for 5 min, no product was formed. As the enzyme still showed 75% activity after 5 min plasma exposure (Figure S13 in the Supporting Information), we attribute the lack of conversion to substrate limitation, possibly caused by poor substrate solubility and insufficient mixing or by evaporation of the ethylbenzene during the treatment.

To overcome the limits of the direct exposure (presumably substrate limitation) but retain the benefit of the in situ approach of keeping the final volume constant, we combined ex situ plasma treatment with the use of immobilized *rAaeUPO* (Figure 8). After the addition of the substrate, a volume of 100  $\mu\text{L}$  of the solution from the liquid column above the beads

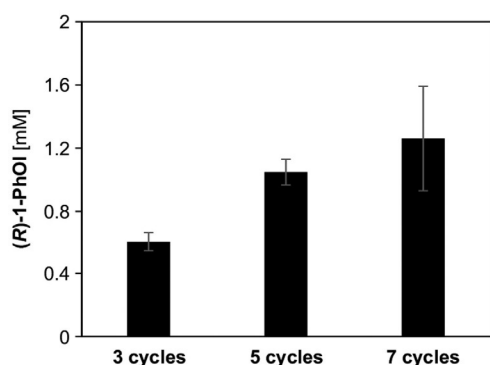


**Figure 8.** Production of (*R*)-1-phenylethanol with immobilized *rAaeUPO* using plasma-treated KPi buffer (250 mM) treated for several cycles. Supernatant of the reaction vial, that is, buffer without enzyme, was treated as mentioned before and added back into the container. This was repeated for several cycles as indicated. Turnover of ethylbenzene to (*R*)-1-phenylethanol was allowed to take place for 30 min after a new cycle was initiated. (*R*)-1-PhOH: (*R*)-1-phenylethanol.

was taken from the vial, treated with the DBD for 5 min, and returned to the reaction. Using this strategy, the same amount of product was obtained as with the addition of plasma-treated buffer, but without diluting the reaction solution. For reactions with poorly soluble substrates, the ex situ treatment of reaction solutions thus presents a viable option, with the decisive advantage of avoiding sample dilution in synthetic applications.

The product obtained using immobilized *rAaeUPO* and several cycles of plasma-treated buffer presented an ee value of  $>99\%$ , indicating that the plasma treatment neither modified nor racemized (*R*)-1-phenylethanol, nor did it change the selectivity of the enzyme. Up to seven treatment cycles were tested, resulting in an accumulation of (*R*)-1-phenylethanol to concentrations of up to 1.26 mM, which is in the range of product obtained with 60 min cumulated treatment time in the ex situ approach (Table 1). To investigate whether the immobilized *rAaeUPO* that had been exposed to plasma-treated liquids could be reused, we extracted the supernatant before new plasma-treated buffer and substrate were added. In all of the eight cycles the same amount of (*R*)-1-phenylethanol was generated (Figure S15, Supporting Information), indicating that enzyme activity is not impaired by repeated exposure to plasma-treated buffer.

## Conclusions

In this work, we have presented the first noninvasive in situ method for the generation of  $\text{H}_2\text{O}_2$  for biocatalysis using a cold plasma device. The advantage of this system is the ability to fine-tune the  $\text{H}_2\text{O}_2$  production rate without changing the setup. We have shown that limitations in enzyme stability under direct plasma treatment of the reaction solution can be overcome by enzyme immobilization. Plasma-driven biocatalysis may present a path forward for peroxidase- and peroxygenase-catalyzed stereoselective oxyfunctionalization reactions. Furthermore, our results suggest that enzyme immobilization is a useful tool for studying the interaction mechanisms of plasma, liquids, and proteins.

## Experimental Section

### Enzymes

HRP was purchased from Sigma (P8375,  $RZ > 2.5$ ) and stored in 100 mM KPi (pH 6.5). SodA (Uniprot P00448) was obtained from an *E. coli* strain harboring a His6-*sodA* fusion plasmid (*E. coli* BL21 DE3 pASK-IBA+::his6-*sodA*) by following standard protocols for cultivation, cell lysis, and purification as described in the Supporting Information. *rAaeUPO* (Uniprot B9W4V6) was purified as described previously.<sup>[61]</sup> Briefly, culture supernatant of a *Pichia pastoris* strain expressing *rAaeUPO* and secreting it into the culture medium was subjected to microfiltration prior to use.

### Plasma source and treatment

The plasma source used for all experiments was the CINOGY PlasmaDerm system (CINOGY, Duderstadt, Germany). For a detailed

review of the plasma source, including power calculations, see Ref. [33]. Unless indicated otherwise, all plasma treatments were performed with standard conditions at room temperature and in ambient air (electrode diameter: 20 mm; pulse amplitude: 13.5 kV; trigger frequency: 300 Hz). Plasma exposure of liquid samples of 110  $\mu\text{L}$  volume was performed using PTFE-coated glass slides. Because plasma treatment increases the hydrophilicity of the glass surface, the liquid was contained in PTFE wells to prevent spreading. The distance between dielectric and sample apex was kept constant at approximately 2 mm for all samples. All subsequent analyses were performed immediately after treatment unless noted otherwise.

### H<sub>2</sub>O<sub>2</sub> measurement

Samples were analyzed and calibrated with a commercially available test kit following the manufacturer's instructions (Spectroquant Hydrogen Peroxide, Merck). After a 10 min reaction time, absorption at 455 nm was measured. Calibration was performed with serial dilutions from 0–200  $\mu\text{M}$  made from H<sub>2</sub>O<sub>2</sub> stock.

### Ex situ activity assays

HRP was added to a guaiacol solution in 100 mM KPi (pH 6.5). To start the reaction, the same volume of 1 mM H<sub>2</sub>O<sub>2</sub> was added and the absorption at 470 nm immediately monitored with a plate reader (Biotek  $\mu\text{Quant}$ , Bad Friedrichshall, Germany). Final concentrations were usually 0.1 U mL<sup>-1</sup> HRP, 5 mM guaiacol, 50 mM KPi, and 0.5 mM H<sub>2</sub>O<sub>2</sub>. For rAaeUPO activity measurements, 2,2'-azino-bis(3-ethylbenzothiazoline-6-sulphonic acid) (ABTS) was used as chromogenic substrate. Final concentrations in this case were 40 nM rAaeUPO, 2.5 mM ABTS, 50 mM sodium acetate buffer (pH 5.5), and 1 mM H<sub>2</sub>O<sub>2</sub>. Activity was determined based on the slope of the linear region of the absorption measurement plot.

### CD spectroscopy

HRP was treated as described above and mixed immediately with four parts of 100 mM KPi. After transfer to a cuvette, CD spectra were recorded with a Jasco J-815 CD spectrometer (Jasco, Pfungstadt, Germany) with the following parameters: range: 190–300 nm; data interval: 0.1 nm; bandwidth: 2 nm; accumulations: 5. KPi buffer was used as a blank. Samples were then extracted from the cuvette and subjected to a Bradford assay performed according to the manufacturer's instructions (RotiNanoquant Kit, Roth, Karlsruhe, Germany). The ellipticity was corrected for the protein concentration as described previously.<sup>[62]</sup>

### Immobilization

HRP and rAaeUPO were immobilized with Relizyme HA403 M beads (Resindion, Binasco, Italy). To this end, the beads (10 mg) were activated by incubation in KPi buffer (pH 7) with 0.4% glutaraldehyde for 1 h. After washing twice with deionized water, the enzyme (up to 5 mg) was added to 1 mL buffer. Immobilization was performed overnight at room temperature under constant shaking. The binding efficiency was determined by measuring the protein concentration in the supernatant after incubation, and was found to be > 80% in all cases.

### Analysis of rAaeUPO catalysis products

Buffer volumes of 110  $\mu\text{L}$  were treated with the DBD plasma as described for HRP for different amounts of time. The treated buffer was then allowed to rest for 5 min for short-lived reactive species to react. This treated buffer (100  $\mu\text{L}$ ) was combined with ethylbenzene (5  $\mu\text{L}$ ) and 1  $\mu\text{M}$  rAaeUPO solution (50  $\mu\text{L}$ ) and incubated for 10 min at 30 °C and 600 rpm. Then, another portion (100  $\mu\text{L}$ ) of treated buffer was added and the reaction was incubated for another 10 min. This was followed by a third addition of treated buffer and incubation. The final reaction volume (355  $\mu\text{L}$ ) was extracted with 300  $\mu\text{L}$  ethyl acetate containing 2 mM 1-octanol as injection standard. The organic phase was dried with MgSO<sub>4</sub> and measured with a Shimadzu 20101 system containing a Hydrodex  $\beta$ -6TBDM column (Macherey–Nagel, Germany). The column was heated at 120 °C for 20 min. Final concentrations of (*R*)-1-phenylethanol were determined by applying a standard curve that was measured with racemic 1-phenylethanol.

### Acknowledgements

We thank Cinogy for kindly providing the plasma source and Britta Schubert for technical assistance. We gratefully acknowledge funding by the German Research foundation to JEB (CRC1316-1 and BA 4193/7-1).

### Conflict of interest

Patent applications have been filed: J. Bandow, A. Yayci, M. Krewing, R. Kourist, A. Gómez Baraibar. Plasma-driven Biocatalysis (International patent application PCT/EP2019/065220, 11.06.2019) J. Bandow, A. Yayci, M. Krewing, R. Kourist, A. Gómez Baraibar. Plasmagetriebene Biokatalyse (German patent application 10 2018 116 052.6, 03.07.2018)

**Keywords:** biocatalysis · peroxidase · peroxides · peroxygenase · plasma chemistry

- [1] E. R. Fisher, *Plasma Processes Polym.* **2004**, *1*, 13.
- [2] R. Morent, N. Geyter, T. Desmet, P. Dubruel, C. Leys, *Plasma Processes Polym.* **2011**, *8*, 171.
- [3] B. Haertel, T. Woedtke, K.-D. Weltmann, U. Lindequist, *Biomol. & Ther.* **2014**, *22*, 477; *Ther.* **2014**, *22*, 477.
- [4] Y. Sakiyama, D. B. Graves, H.-W. Chang, T. Shimizu, G. E. Morfill, *J. Phys. D* **2012**, *45*, 425201.
- [5] F. Judée, S. Simon, C. Bailly, T. Dufour, *Water Res.* **2018**, *133*, 47.
- [6] S. Sasaki, T. Nishida, Y. Tsutsumi, R. Kondo, *FEBS Lett.* **2004**, *562*, 197.
- [7] B. S. van der Veen, M. P. J. Winther, P. Heeringa, *Antioxid. Redox Signaling* **2009**, *11*, 2899.
- [8] B. N. Tripathi, I. Bhatt, K.-J. Dietz, *Protoplasma* **2009**, *235*, 3.
- [9] B. O. Burek, S. Bormann, F. Hollmann, J. Z. Bloh, D. Holtmann, *Green Chem.* **2019**, *21*, 3232.
- [10] B. Valderrama, M. Ayala, R. Vazquez-Duhalt, *Chem. Biol.* **2002**, *9*, 555.
- [11] D. Jung, C. Streb, M. Hartmann, *Microporous Mesoporous Mater.* **2008**, *113*, 523.
- [12] Y. Ni, E. Fernández-Fueyo, A. Gomez Baraibar, R. Ullrich, M. Hofrichter, H. Yanase, M. Alcalde, W. J. H. van Berkel, F. Hollmann, *Angew. Chem. Int. Ed.* **2016**, *55*, 798; *Angew. Chem.* **2016**, *128*, 809.
- [13] M. Girhard, E. Kunigk, S. Tihovsky, V. V. Shumyantseva, V. B. Urlacher, *Bio-technol. Appl. Biochem.* **2013**, *60*, 111.
- [14] I. Zachos, S. K. Gassmeyer, D. Bauer, V. Sieber, F. Hollmann, R. Kourist, *Chem. Commun.* **2015**, *51*, 1918.

- [15] D. I. Perez, M. M. Grau, I. W. C. E. Arends, F. Hollmann, *Chem. Commun.* **2009**, 6848.
- [16] Y. Shiraiishi, S. Kanazawa, D. Tsukamoto, A. Shiro, Y. Sugano, T. Hirai, *ACS Catal.* **2013**, *3*, 2222.
- [17] W. Zhang, B. O. Burek, E. Fernández-Fueyo, M. Alcalde, J. Z. Bloh, F. Hollmann, *Angew. Chem. Int. Ed.* **2017**, *56*, 15451; *Angew. Chem.* **2017**, *129*, 15654.
- [18] S. J.-P. Willot, E. Fernández-Fueyo, F. Tieves, M. Pesic, M. Alcalde, I. W. C. E. Arends, C. B. Park, F. Hollmann, *ACS Catal.* **2019**, *9*, 890.
- [19] K. Lee, S.-H. Moon, *J. Biotechnol.* **2003**, *102*, 261.
- [20] C. Kohlmann, S. Lütz, *Eng. Life Sci.* **2006**, *6*, 170.
- [21] A. E. W. Horst, S. Bormann, J. Meyer, M. Steinhagen, R. Ludwig, A. Drews, M. Ansorge-Schumacher, D. Holtmann, *J. Mol. Catal. B: Enzym.* **2016**, *133*, 137–142.
- [22] T. Krieg, S. Hüttmann, K.-M. Mangold, J. Schrader, D. Holtmann, *Green Chem.* **2011**, *13*, 2686.
- [23] V. V. Kovačević, B. P. Dojčinović, M. Jović, G. M. Roglić, B. M. Obradović, M. M. Kuraica, *J. Phys. D* **2017**, *50*, 155205.
- [24] P. Rajasekaran, P. Mertmann, N. Bibinov, D. Wandke, W. Viöl, P. Awakowicz, *Plasma Processes Polym.* **2010**, *7*, 665.
- [25] Y. Wang, D. Lan, R. Durrani, F. Hollmann, *Curr. Opin. Chem. Biol.* **2017**, *37*, 1.
- [26] N. C. Veitch, *Phytochemistry* **2004**, *65*, 249.
- [27] G. I. Berglund, G. H. Carlsson, A. T. Smith, H. Szöke, A. Henriksen, J. Hajdu, *Nature* **2002**, *417*, 463.
- [28] F. W. Krainer, A. Glieder, *Appl. Microbiol. Biotechnol.* **2015**, *99*, 1611.
- [29] J.-W. Lackmann, S. Baldus, E. Steinborn, E. Edengeiser, F. Kogelheide, S. Langklotz, S. Schneider, L. I. O. Leichert, J. Benedikt, P. Awakowicz et al., *J. Phys. D: Appl. Phys.* **2015**, *48*, 494003.
- [30] Z. Ke, Q. Huang, *Plasma Processes Polym.* **2013**, *10*, 731.
- [31] P. Attri, N. Kumar, J. H. Park, D. K. Yadav, S. Choi, H. S. Uhm, I. T. Kim, E. H. Choi, W. Lee, *Sci. Rep.* **2015**, *5*, 8221.
- [32] J. de Backer, J. Razzokov, D. Hammerschmid, C. Mensch, Z. Hafideddine, N. Kumar, G. van Raemdonck, M. Yusupov, S. van Doorslaer, C. Johannessen, F. Sobott, A. Bogaerts, S. Dewilde, *Redox Biol.* **2018**, *19*, 1–10.
- [33] M. Kuchenbecker, N. Bibinov, A. Kaemling, D. Wandke, P. Awakowicz, W. Viöl, *J. Phys. D* **2009**, *42*, 45212.
- [34] M. Krewing, J. J. Stepanek, C. Cremers, J.-W. Lackmann, B. Schubert, A. Müller, P. Awakowicz, L. I. O. Leichert, U. Jakob, J. E. Bandow, *J. R. Soc. Interface* **2019**, *16*, 20180966.
- [35] M. Farasat, S. Arjmand, S. O. R. Siadat, Y. Sefidbakht, H. Ghomi, *Sci Rep* **2018**, *8*, 16647.
- [36] E. Nagababu, J. M. Rifkind, *Biochemistry* **2000**, *39*, 12503.
- [37] E. Nagababu, J. M. Rifkind, *Antioxid. Redox Signaling* **2004**, *6*, 967.
- [38] J. J. P. Perry, D. S. Shin, E. D. Getzoff, J. A. Tainer, *Biochim. Biophys. Acta* **2010**, *1804*, 245.
- [39] Y. Sheng, I. A. Abreu, D. E. Cabelli, M. J. Maroney, A.-F. Miller, M. Teixeira, J. S. Valentine, *Chem. Rev.* **2014**, *114*, 3854.
- [40] T. Li, H. L. Bonkovsky, J.-t. Guo, *BMC Struct. Biol.* **2011**, *11*, 13.
- [41] H. Zhang, Z. Xu, J. Shen, X. Li, L. Ding, J. Ma, Y. Lan, W. Xia, C. Cheng, Q. Sun et al., *Sci. Rep.* **2015**, *5*, 10031.
- [42] S. Choi, P. Attri, I. Lee, J. Oh, J.-H. Yun, J. H. Park, E. H. Choi, W. Lee, *Sci. Rep.* **2017**, *7*, 1027.
- [43] T. R. Brubaker, K. Ishikawa, K. Takeda, J.-S. Oh, H. Kondo, H. Hashizume, H. Tanaka, S. D. Knecht, S. G. Bilén, M. Hori, *J. Appl. Phys.* **2017**, *122*, 213301.
- [44] M. Krewing, B. Schubert, J. E. Bandow, *Plasma Chemistry and Plasma Processing* **2019**, <https://doi.org/10.1007/s11090-019-10053-2>.
- [45] S. Goldstein, G. Czapski, *Int. J. Radiat. Biol. Relat. Stud. Phys. Chem. Med.* **1984**, *46*, 725.
- [46] C. Klinkhammer, C. Verlackt, D. śmiłowicz, F. Kogelheide, A. Bogaerts, N. Metzler-Nolte, K. Stapelmann, M. Havenith, J.-W. Lackmann, *Sci. Rep.* **2017**, *7*, 13828.
- [47] S. K. Pankaj, N. N. Misra, P. J. Cullen, *Innovative Food Sci. Emerging Technol.* **2013**, *19*, 153.
- [48] I. Bekard, D. E. Dunstan, *Soft Matter* **2014**, *10*, 431.
- [49] K. Stapelmann, J.-W. Lackmann, I. Buerger, J. E. Bandow, P. Awakowicz, *J. Phys. D* **2014**, *47*, 85402.
- [50] P. J. Bruggeman, M. J. Kushner, B. R. Locke, J. G. E. Gardeniers, W. G. Graham, D. B. Graves, R. C. H. M. Hofman-Caris, D. Maric, J. P. Reid, E. Ceriani et al., *Plasma Sources Sci. Technol.* **2016**, *25*, 53002.
- [51] M. Okuda, T. Tsuruta, K. Katayama, *Phys. Chem. Chem. Phys.* **2009**, *11*, 2287.
- [52] X. Lu, G. V. Naidis, M. Laroussi, S. Reuter, D. B. Graves, K. Ostrikov, *Phys. Rep.* **2016**, *630*, 1.
- [53] P. Attri, Y. H. Kim, D. H. Park, J. H. Park, Y. J. Hong, H. S. Uhm, K.-N. Kim, A. Fridman, E. H. Choi, *Sci. Rep.* **2015**, *5*, 9332.
- [54] F.-J. Schmitt, G. Renger, T. Friedrich, V. D. Kreslavski, S. K. Zharmukhamedov, D. A. Los, V. V. Kuznetsov, S. I. Allakhverdiev, *Biochim. Biophys. Acta* **2014**, *1837*, 835.
- [55] W. Zhang, E. Fernández-Fueyo, Y. Ni, M. van Schie, J. Gacs, R. Renirie, R. Wever, F. G. Mutti, D. Rother, M. Alcalde et al., *Nat. Catal.* **2018**, *1*, 55.
- [56] M. Kluge, R. Ullrich, K. Scheibner, M. Hofrichter, *Green Chem.* **2012**, *14*, 440.
- [57] M. J. Pecyna, R. Ullrich, B. Bittner, A. Clemens, K. Scheibner, R. Schubert, M. Hofrichter, *Appl. Microbiol. Biotechnol.* **2009**, *84*, 885.
- [58] P. Molina-Espeja, E. Garcia-Ruiz, D. Gonzalez-Perez, R. Ullrich, M. Hofrichter, M. Alcalde, *Appl. Environ. Microbiol.* **2014**, *80*, 3496.
- [59] J. L. Lepe-Zuniga, J. S. Zigler, I. Gery, *J. Immunol. Methods* **1987**, *103*, 145.
- [60] M. Kirsch, E. E. Lomonosova, H.-G. Korth, R. Sustmann, H. Groot, *J. Biol. Chem.* **1998**, *273*, 12716.
- [61] P. Molina-Espeja, S. Ma, D. M. Mate, R. Ludwig, M. Alcalde, *Enzyme Microb. Technol.* **2015**, *73–74*, 29.
- [62] P. C. F. Graf, M. Martinez-Yamout, S. VanHaerents, H. Lillie, H. J. Dyson, U. Jakob, *J. Biol. Chem.* **2004**, *279*, 20529.

---

Manuscript received: December 16, 2019

Revised manuscript received: February 4, 2020

Accepted manuscript online: February 5, 2020

Version of record online: March 18, 2020